Dismutation of a Molybdenum(IV) Acetonitrile−NNH_2 Complex to a Molybdenum(IV) Ethylimido Complex + N_2: Mechanistic Implications on the Protonation of Coordinated Nitriles at the β-Carbon Atom

Chinnappan Sivasankar, Natascha Böres, Gerhard Peters, Carsten M. Habeck, Felix Studt, and Felix Tuczek*

Institut für Anorganische Chemie, Christian-Albrechts-Universität Kiel, D-24098 Kiel, Germany

Received March 22, 2005

Reaction of the Mo(0) depe complex $[Mo(N_2H_2)(depe)_2(CH_3CN)](OTf)_2$ (**3**) (depe = 1,2-bis(diethylphosphino)ethane) with base gives the ethylimido complex $[Mo(depe)_2(CH_3CH_2N)(CH_3CN)](OTf)_2$ (**10**), whereas base treatment of the corresponding dppe complex $[Mo(N_2H_2)(dppe)_2(OTf)](OTf)$ (**12**; dppe = 1,2-bis(diphenylphosphino)ethane) leads to formation of $[Mo(N_2)(dppe)_2(CH_3CN)]$ (**14**). Reaction of dinitrogen complex **14** with HBF_4 gives the ethylimido complex $[Mo(dppe)_2(CH_3CH_2N)(F)](BF_4)$ (**17**). The protonation of coordinated acetonitrile in complexes **3** and **14** giving the corresponding ethylimido complexes is investigated. Experimental and theoretical evidence is presented for the hypothesis that acetonitrile is only activated toward protonation at the β-carbon if it is bound along with a Lewis base like triflate or fluoride to a Mo(0) center. The activation is further influenced by the phosphine coligands (depe > dppe). DFT geometry optimizations show that the acetonitrile ligand is bent in the activated complexes, exhibiting a lone pair at C_β. Protonation at this position first leads to Mo(II) methyl-azavinylidene intermediates (which cannot be isolated) and then to Mo(IV) ethylimido complexes.

I. Introduction

The metal-centered conversion of dinitrogen to ammonia under ambient conditions has been an issue of long-standing interest.[1] Before the discovery of a Mo(III) triamidoamine system providing the first truly catalytic process of ammonia synthesis proceeding via well-defined intermediates,[2] this chemistry has been a domain of Mo and W complexes with diphosphine (depe or dppe) ligands.[1,3,4] For $[M(N_2)_2(dppe)_2]$ complexes (M = Mo, W), one dinitrogen can be exchanged in a photochemical reaction against a nitrile ligand, leading to *trans*-$[M(N_2)(RCN)(dppe)_2]$ systems.[5,6] As evident from spectroscopic data and theoretical calculations, the N_2 ligand is more highly activated in the *trans*-nitrile than in the parent bis(dinitrogen) complexes,[5−7] facilitating protonation to the corresponding NNH_2 species. Remarkably, this protonation proceeds under retention of the $(dppe)_2$−nitrile ligation. This is in contrast to corresponding bis(dinitrogen) complexes, where upon treatment with acids HX, one N_2 ligand is exchanged against the conjugate base of the acid X, leading to $[M(NNH_2)X(diphos)_2]^+$ systems (M = Mo, W; diphos = dppe, depe).[1,3−9] With respect to the construction of a catalytic system for N_2 fixation, this is unfavorable, as it corresponds to 50% loss of activated substrate.

trans-Nitrile dinitrogen complexes thus have a double advantage over their bis(dinitrogen) counterparts: higher activation and retention of the *trans* ligand upon protonation. Unfortunately, however, the photochemical method to generate the dppe *trans*-nitrile dinitrogen systems does not appear to be applicable to the synthesis of the corresponding depe complexes.[10] Obviously the quantum yield for the photosubstitution reaction of the bis(dinitrogen) compounds leading to $[M(N_2)(RCN)(diphos)_2]$ (M = Mo, W; diphos = dppe, depe) is much lower for $[M(N_2)_2(depe)_2]$ than for $[M(N_2)_2(dppe)_2]$. This is possibly due to the fact that the relatively intense, broad CT band at 380 nm characteristic of the Mo/W dppe systems is lacking for the depe analogues.[11] On the other hand, the complexes $[M(N_2)(RCN)(depe)_2]$ (M

* Corresponding author. E-mail: ftuczek@ac.uni-kiel.de. Fax: +49 431 880 1520.

(1) (a) MacKay, B. A.; Fryzuk, M. D. *Chem. Rev.* **2004**, *104*, 385. (b) Barriere, F. *Coord. Chem. Rev*. **2003**, *236*, 71. (c) Hidai, M. *Coord. Chem. Rev.* **1999**, *185−186*, 99−108. (d) Hidai, M.; Mizobe, Y. *Chem. Rev.* **1995**, *95*, 1115. (e) Leigh, G. J. *Acc. Chem. Res.* **1992**, *25*, 177. (f) Henderson, R. A. *Transition Met. Chem.* **1990**, *15*, 330.

(2) (a) Studt, F.; Tuczek, F. *Angew. Chem., Int. Ed.* **2005**, *44*, 5639. (b) Yandulov, D. V.; Schrock, R. R. *Inorg. Chem.* **2005**, *44*, 1103. (c) Ritleng, V.; Yandulov, D. V.; Weare, W. W.; Schrock, R. R.; Hock, A. S.; Davis, W. M. *J. Am. Chem. Soc.* **2004**, *126* (19), 6150. (d) Yandulov, D. V.; Schrock, R. R. *Science* **2003**, *301*, 76. (e) Yandulov, D. V.; Schrock, R. R.; Rheingold, A. L.; Cecciavelli, C.; Davis, W. M. *Inorg. Chem.* **2003,** *42*, 796. (f) Yandulov, D. V.; Schrock, R. R. *J. Am. Chem. Soc.* **2002**, *124*, 6252.

(3) Henderson, R. A.; Leigh, G. J.; Pickett, C. *Adv. Inorg. Chem. Radiochem.* **1983**, *27*, 197.

(4) Chatt, J.; Dilworth, J. R.; Richards, J. R. *Chem. Rev.* **1978**, *78*, 589.

(5) Chatt, J.; Leigh, G. J.; Neukomm, H.; Pickett, C. J.; Stanley, D. R. *J. Chem. Soc., Dalton Trans*. **1980**, 121.

(6) Tatsumi, T.; Hidai, M.; Uchida, Y. *Inorg. Chem*. **1975**, *14*, 2530.

(7) Habeck, C. M.; Lehnert, N.; Näther, C.; Tuczek, F. *Inorg. Chem. Acta* **2002**, *337*, 11.

(8) Dilworth, J. R.; Richards, R. L. *Inorg. Synth.* **1980**, *20*, 119.

(9) (a) Chatt, J.; Pearman, A. J.; Richards, R. L. *J. Chem. Soc., Dalton Trans.* **1976**, 1520. (b) Chatt, J.; Pearman, A. J.; Richards, R. L. *J. Chem. Soc., Dalton Trans.* **1977**, 1852.

(10) Habeck, C. M.; Böres, N.; Tuczek, F. Unpublished work.

(11) Lehnert, N.; Tuczek, F. *Inorg. Chem.* **1999**, *38*, 1671.

10.1021/om050220r CCC: $30.25
Publication on Web 09/24/2005

Scheme 1

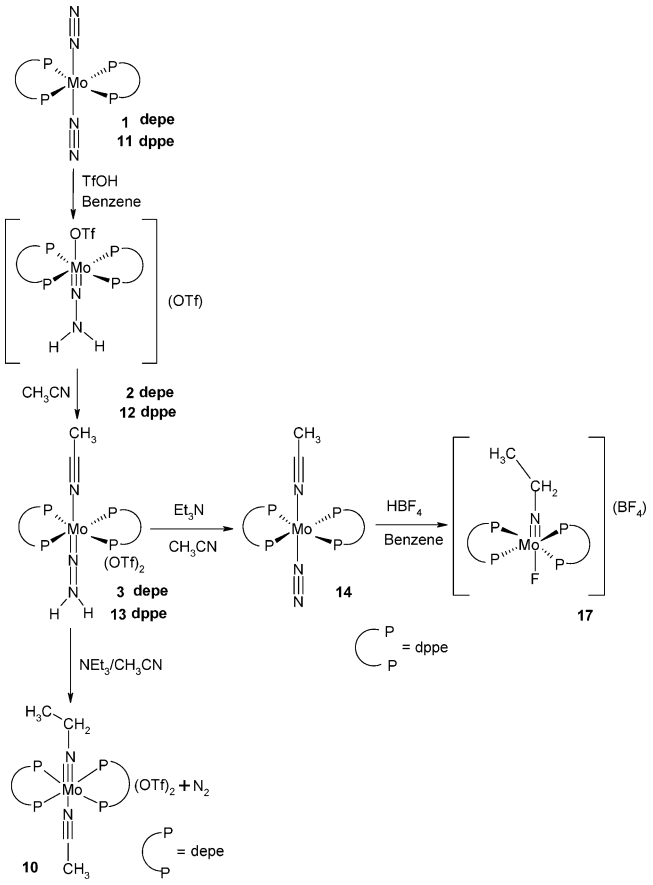

= Mo, W) potentially are of high interest to synthetic nitrogen fixation, as the dinitrogen ligand should be even more activated than in the corresponding dppe compounds.[7] It therefore would be desirable to have a general (possibly non-photochemical) method for the synthesis of *trans* nitrile-dinitrogen complexes that is applicable to both dppe and depe systems.

In this respect the finding of Field et al. is remarkable in which the complex *trans*-$[W(N_2)(CH_3CN)(dppe)_2]$ can in fact be obtained via a sequence of thermal reaction steps.[12] Of key importance in this reaction route is the choice of triflic acid, HOTf, to protonate $[W(N_2)_2(dppe)_2]$, generating $[W(NNH_2)(OTf)(dppe)_2](OTf)$. The triflate ligand in this NNH_2 complex is easily displaced in acetonitrile, leading to $[W(NNH_2)(RCN)(dppe)_2](OTf)_2$. Deprotonation of this complex with base (NEt_3 or KO^t-Bu) then generates the acetonitrile-N_2 complex $[W(N_2)(CH_3CN)(dppe)_2]$. The first objective of the present paper was to apply this method to generate the corresponding complexes with depe ligands, i.e., $[M(N_2)(RCN)(depe)_2]$ (M = Mo, W). For practical reasons, we focused our attention on the Mo system.[13] Up to the complex $[Mo(NNH_2)(CH_3CN)(depe)_2](OTf)_2$ (**3**) we found the Mo depe chemistry to be analogous to that of the W dppe system (Scheme 1). Surprisingly, however, treatment of **3** with base did not lead to the corresponding N_2-CH_3CN complex but to formation of the Mo(IV) ethylimido complex $[Mo(CH_3CH_2N)(CH_3CN)(depe)_2](OTf)_2$ (**10**). As evolution of N_2 was observed upon addition of base, this reaction in fact corresponds to a *dismutation* of an NNH_2-CH_3CN complex to N_2 + coordinated ethylimide. We further found that this reaction does not require stoichiometric, but only catalytic amounts of base. It even proceeds spontaneously in the absence of base, however at a slower rate.

Protonation of coordinated nitriles at the β-carbon atom to generate alkylimido complexes has been evidenced before.[12,14,15] In particular, Field et al. in the above-mentioned study showed that $[W(N_2)(CH_3CN)(dppe)_2]$ can be protonated with HBF_4 to the ethylimido complex $[WF(CH_3CH_2N)(dppe)_2]BF_4$. The same observation has been made by Hidai et al. for Mo and W complexes with various nitrile ligands.[15] These authors also provided a mechanism for the protonation of coordinated β-ketonitriles and their subsequent C−N cleavage. To the best of our knowledge, however, no mechanism for the protonation of simple aliphatic and aromatic nitriles on transition-metal complexes has been given. The purpose of the present paper therefore is to explain the observed base-catalyzed dismutation of the Mo NNH_2−acetonitrile complex to Mo(IV) ethylimide + N_2 in the framework of a general mechanism for the protonation of coordinated nitriles at the β-atom. To this end, the dismutation reaction is presented first, providing extensive characterization of the corresponding intermediates. Then, various mechanistic scenarios are explored to account for the experimental observations, and the most probable reaction pathway is identified with the help of DFT. The corresponding mechanism is finally applied to the protonation of a mixed acetonitrile−N_2 complex with HBF_4. The general implications of these results are discussed.

2. Experimental Results

2.1. Synthesis of $[Mo(N_2H_2)(depe)_2(OTf)](OTf)$ (2) and Reaction with Acetonitrile. The NNH_2 complex $[Mo(N_2H_2)(depe)_2(OTf)](OTf)$ (**2**) was prepared by reaction of the bis(dinitrogen) complex $[Mo(N_2)_2(depe)_2]$ (**1**) with triflic acid (Scheme 1).[16] The ^1H NMR spectrum of complex **2** shows peaks at 1.24 and 2.06 ppm for the CH_3 and CH_2 protons of the depe ligand, respectively; a peak at 8.46 ppm corresponds to the NH_2 protons (Table 1). ^{31}P NMR of complex **2** displays a single peak at 47.06 ppm for the depe phosphorus atoms, indicating a *trans* geometry of the complex. ^{19}F NMR of complex **2** shows two peaks, one at −78.89 ppm for the coordinated, and one (1:1 ratio) at −79.65 ppm for the noncoordinated OTf fluorine atom. The IR spectrum exhibits two bands for the NH_2 stretches at 3097 and 3251 cm^{-1} (Table 2).

(12) Field, L. D.; Jones, N. G.; Turner, P. *Organometallics* **1998**, *17*, 2394.

(13) (a) Tuczek, F.; Horn, K. H.; Lehnert, N. *Coord. Chem. Rev.* **2003**, *245*, 107. (b) Lehnert, N.; Tuczek, F. *Inorg. Chem.* **1999**, *38*, 1659.

(14) (a) Sónia, M. P.; Cunha, R. M.; Fátima, M.; Guedes da Silva, C.; Pombeiro, A. J. L. *Inorg. Chem.* **2003**, *42*, 2157. (b) Guedes da Silva, M. F. C.; Fraústo da Silva, J. J. R.; Pombeiro, A. J. L. *Inorg. Chem.* **2002**, *41*, 219. (c) Fraústo da Silva, J. J. R.; Guedes da Silva, M. F. C.; Henderson, R. A.; Pombeiro, A. J. L.; Richards, R. L. *J. Organomet. Chem.* **1993**, *461*, 141. (d) Pombeiro, A. J. L. *New J. Chem.* **1994**, *18*, 163. (e) Pombeiro, A. J. L. *Inorg. Chim. Acta* **1992**, *198*−*200*, 179. (f) Pombeiro, A. J. L.; Hughes, D. L.; Richards, R. L. *J. Chem. Soc., Chem. Commun.* **1988**, 1052.

(15) (a) Tanabe, Y.; Seino, H.; Ishii, Y.; Hidai, M. *J. Am. Chem. Soc.* **2000**, *122*, 1690. (b) Seino, H.; Tanabe, Y.; Ishii, Y.; Hidai, M. *Inorg. Chim. Acta* **1998**, *280*, 163.

(16) Hussain, W.; Leigh, G. J.; Ali, H. M.; Pickett, C. J.; Rankin, D. A. *J. Chem. Soc., Dalton Trans.* **1984**, 1703.

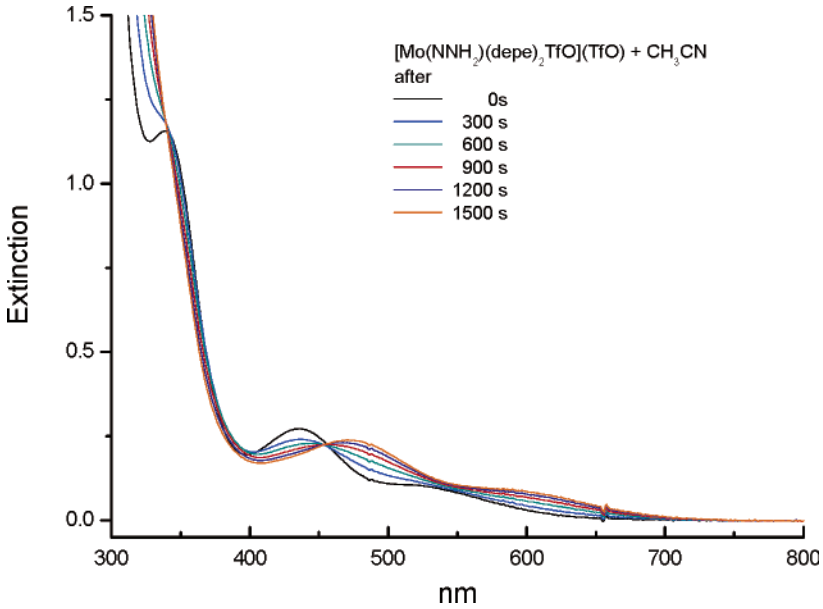

Figure 1. UV−visible spectroscopic monitoring of the conversion of $[Mo(depe)_2(NNH_2)(OTf)]^+$(**2**) to $[Mo(depe)_2(NNH_2)(CH_3CN)]^{2+}$ (**3**).

Table 1. ^{1}H NMR, ^{31}P NMR, and ^{19}F NMR Spectral Data (δ, ppm) of Complexes 2, 3, 10, 14, and 17

		^{1}H NMR								^{31}P NMR		
system	solvent	CH_3 acetonitrile	CH_3 depe	CH_2 depe	CH_2 dppe	Ph dppe	NH_2 NNH_2	CH_2 NEt	CH_3 NEt	depe, dppe	^{19}F NMR	
2	THF-d_8		1.24	2.06						47.06	−78.89 (bonded)	−79.65 (free)
3	CD_3CN	2.18	1.16	1.92			7.43			47.27		−79.60 (free)
10	CD_3CN	1.9	1.20	2.05				0.86	1.0	45.96		
14	C_6D_6	0.98			2.35	6.89−7.57				59.9		
17	CD_2Cl_2				2.60 2.71	6.86−7.43		1.83	−0.19	46.45	−148.31 (Mo−F)	−77.86 (BF_4)

In analogy with the dppe complex $[W(NNH_2)(dppe)_2(OTf)](OTf)$,[12] the coordinated triflate of **2** is replaced by acetonitrile upon stirring in CH_3CN at room temperature, leading to $[Mo(NNH_2)(depe)_2(CH_3CN)](OTf)_2$ (**3**) (Scheme 1). The ligand exchange reaction can be followed by UV−visible spectroscopy (Figure 1). Complex **2** shows three absorption bands, at 340, 434, and 540 nm. After 25 min these bands disappear, giving rise to new bands at 479 and 600 nm, which indicate formation of complex **3**. ^{19}F NMR of the product **3** shows a single peak at −79.6 ppm corresponding to noncoordinated OTf and thus reveals that the bound OTf anion has been replaced by acetonitrile (Table 1). The ^{31}P NMR spectrum of **3** displays a single peak at 47.27 ppm, indicating that all four depe phosphorus atoms are equivalent and a *trans* configuration of the NNH_2 and CH_3CN ligands applies. ^{1}H NMR of complex **3** shows peaks at 1.16 and 1.92 ppm for the CH_3 and CH_2 protons of depe, respectively, a peak at 7.43 ppm for the NNH_2 protons, and a peak at 2.18 ppm for the CH_3 protons of acetonitrile (Table 1, Figure S1). The IR spectrum of **3**, finally, exhibits a band at 1326 cm^{-1} for the N=N stretch and bands at 3095 and 3253 cm^{-1} for N−H vibrations of the NNH_2 group (Table 2). The C≡N stretch of bound acetonitrile appears at 2278 cm^{-1}, slightly higher in energy than in the free ligand.

2.2. Reaction of $[Mo(N_2H_2)(depe)_2(CH_3CN)](OTf)_2$ (3) with Base. Addition of NEt_3 to $[Mo(N_2H_2)(depe)_2(CH_3CN)](OTf)_2$ (**3**) in acetonitrile at room temperature leads to formation of $[Mo(depe)_2(NCH_2CH_3)(CH_3CN)](OTf)_2$ (**10**) under evolution of N_2 (Scheme 1). Successive reduction of the added amount of NEt_3 shows that the base is only required to start this raction. In fact, the reaction was also found to occur spontaneously in the absence of NEt_3. The identity of reaction product **10** was proven by various spectroscopic methods. ^{1}H NMR shows peaks at 0.86 and 1.0 ppm for the CH_3 and CH_2 protons of NCH_2CH_3, respectively, and a peak at 1.9 ppm for the methyl protons of acetonitrile, confirming the simultaneous presence of acetonitrile and alkylimide (Figure S2 (a), Table 1). The peaks at 1.2 and 2.05 ppm are due to the CH_3 and CH_2 protons of depe, respectively. ^{31}P NMR of **10** displays a single peak at 45.96 ppm (Figure S2 (b)), indicating that all four phosphorus atoms from depe are equivalent and the complex has a *trans* configuration. The IR spectrum of **10** exhibits a band at 2280 cm^{-1} for the C≡N stretch (Table 2); a band for the Mo≡N stretch cannot be assigned unambiguously. Although complex **10** crystallizes well from a

Table 2. IR and Raman Spectral Data (cm^{-1}) of Complexes 2, 3, 10, and 14

	stretching frequences		
system	C≡N	N≡N	NH_2
2			3097 (IR) 3251 (IR)
3	2278 (IR)	1326 (IR) (N=N)	3095 (IR) 3253 (IR)
10	2280 (IR) 2272 (Raman)		
14	2199 (IR) 2210 (Raman)	1919 (IR) 1913 (Raman)	

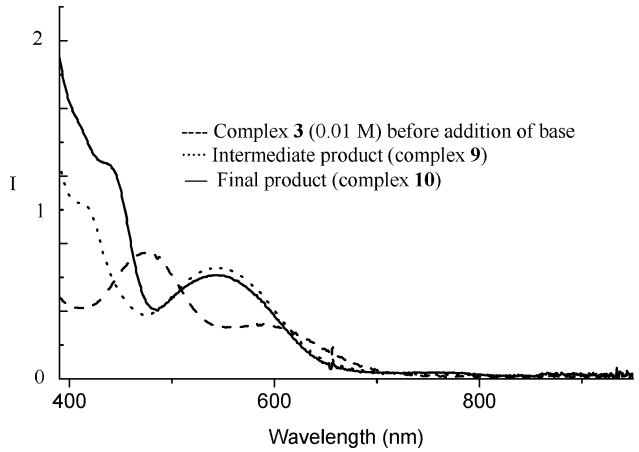

Figure 2. UV−visible spectrum in acetonitrile at room temperature.

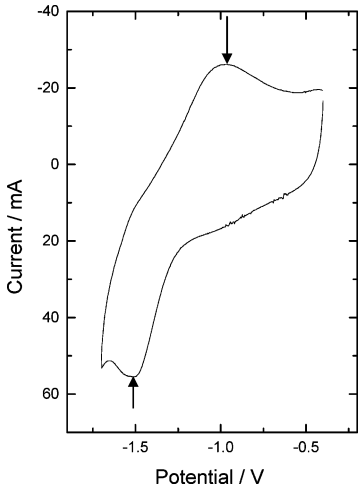

Figure 3. Cyclic voltammogram of complex **10** (1×10^{-4} mol) in acetonitrile at room temperature.

mixture of acetonitrile and diethyl ether, the X-ray structure refinement indicates significant thermal disorder, precluding a single-crystal structure determination.

The base-catalyzed conversion of complex **3** to **10** was also monitored by UV−visible absorption spectroscopy. Electronic spectra recorded before and after addition of base to the acetonitrile solution of complex **3** are shown in Figure 2. Complex **3** exhibits absorption bands centered around 470 and 605 nm. After addition of base these bands disappear immediately and new bands appear at 415 and 548 nm due to the formation of an intermediate (possibly **9**, cf. Scheme 2). Over a period of 0.5 h this intermediate is completely converted to the final product, complex **10**, as indicated by a shift of the 415 nm band to 440 nm. It should be noted that complex **10** is also obtained directly from the reaction of **2** with base in acetonitrile.

Complex **10** was also characterized by cyclic voltammetery performed on a 1×10^{-4} M solution in freshly prepared, degassed acetonitrile containing 0.1 M $[NBu_4](BF_4)$ as supporting electrolyte with a Pt electrode as anode. As evident from Figure 3, reduction takes place at −1.5 V and oxidation at −1.0 V versus ferrocenium−ferrocene. The observed potentials are 0.71 V less negative than values reported for the similar system

Scheme 2

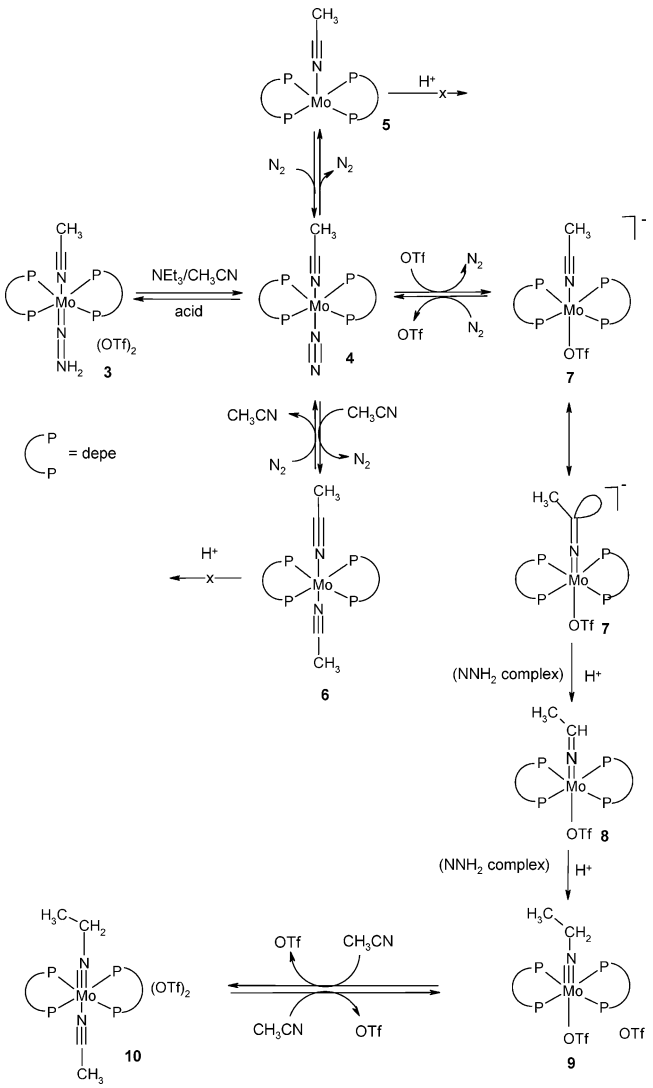

([Mo(dppe)$_2$(NR)(X)]$^+$) in DMF (R = Et, X = Cl),[17] which appears to be due to the absence of a strong donor in *trans* position to the ethylimido ligand in **10**.

2.3. Mechanism of the Formation of [Mo(depe)$_2$(NCH$_2$CH$_3$)(CH$_3$CN)](OTf)$_2$ (10). Scheme 2 displays possible pathways for the reaction of the Mo(IV) acetonitrile−NNH_2 complex **3** with base. In analogy with the corresponding dppe complex **13** (see below) and other NNH_2 systems the addition of base to [Mo(N_2H_2)(depe)$_2$(CH_3CN)](OTf)$_2$ (**3**) in acetonitrile primarily leads to formation of the dinitrogen complex **4** with acetonitrile in *trans* position. In the case of the dppe system the acetonitrile−dinitrogen complex **14** can be isolated after base treatment of the Mo NNH_2 complex (see below and ref 12), whereas for the depe system protonation of acetonitrile and loss of N_2 occur (vide supra). From DFT calculations on a model of **3**, however, the acetonitrile ligand does *not* appear to be activated for protonation at the β-carbon, as this atom carries a fairly large positive charge (+0.56, see below), rather rendering it susceptible to *nucleophilic* attack.[18]

For the possible activation of bound acetonitrile toward protonation at a Mo(0) center, three scenarios

(17) Alias, Y.; Ibrahim, S. K.; Queiros, M. A.; Fonseca, A.; Talarmin, J.; Volant, F.; Pickett, C. J. *J. Chem. Soc., Dalton Trans.* **1997**, 4807.

Scheme 3

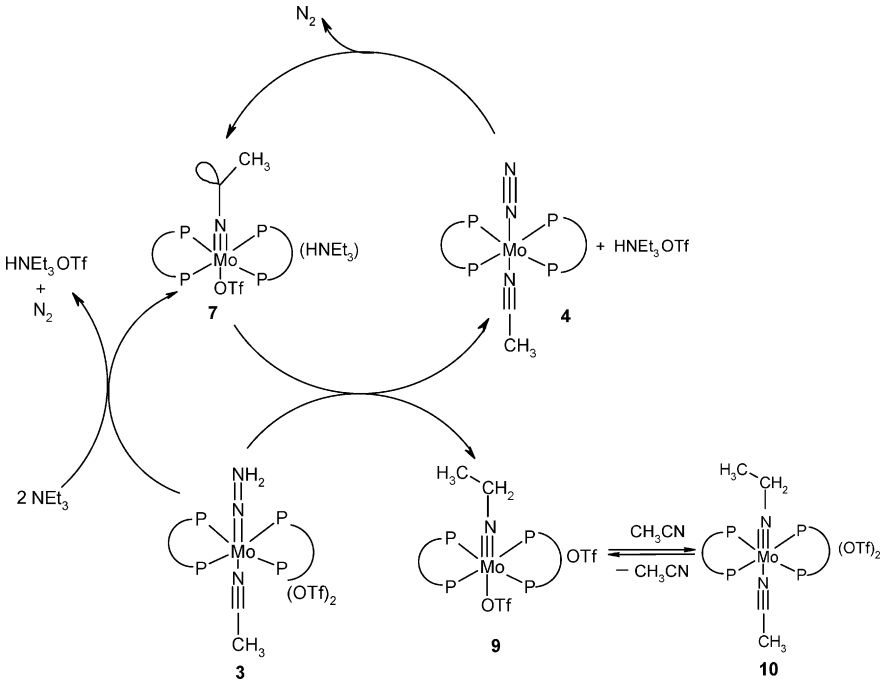

thus can be envisaged (Scheme 2): (i) loss of N_2 leading to the five-coordinate Mo(0) monoacetonitrile complex **5**, (ii) exchange of N_2 against acetonitrile, leading to the Mo(0) bis(acetonitrile) complex **6**; and (iii) exchange of N_2 against triflate, leading to $[Mo(CH_3CN)(OTf)(depe)_2]^-$ (**7**). As shown by DFT, the positive charge on the acetonitrile β-carbon is not changed much in the five-coordinate and bis(acetonitrile) intermediates **5** and **6**, respectively (see below); that is, acetonitrile is not activated for protonation in these systems either. An appreciable reduction of the positive charge on the β-carbon atom of acetonitrile is only observed for the triflate-bound complex **7**, where also a bending of this ligand occurs. Both of these findings indicate an activation of the nitrile toward protonation. Attachment of a proton to the β-carbon atom in a DFT simulation in fact leads to formation of a C−H bond at this position (see below). We therefore conclude that the anionic, base-coordinated intermediate **7** (Scheme 2) is essential for the observed formation of the ethylimido complex **10**. Importantly, complex **10** was also directly obtained from the reaction of **2** with base in acetonitrile (vide supra). In this case, deprotonation of **2** by the added base and exchange of dinitrogen against nitrile also leads to the acetonitrile−triflate complex **7**, which reacts as shown in Scheme 2. The formation of complex **7** is even possible without base from deprotonation of the NNH_2 complex **2** by triflate, followed by replacement of dinitrogen by OTf; this route applies to the *spontaneous* reaction of the NNH_2−triflate complex **2** to the alkylimido complex **10**.

After double protonation of the coordinated nitrile ligand at C_β ultimately leading to **9** (Scheme 2), the bound OTf anion undergoes an exchange reaction with the solvent acetonitrile, and upon crystallization, the alkylimido−acetonitrile complex **10** is obtained. As the reaction occurs with very small amounts of base or even spontaneously, the protonating agent must be the NNH_2 complex **3** itself. The whole reaction therefore can be described as a *dismutation* of **3**, involving an *intermolecular* proton transfer from the NNH_2 group to coordinated acetonitrile under formation of ethylimide and gaseous N_2. A different visualization of the corresponding mechanism is given in Scheme 3. It shows that the reaction is started by addition of very small amounts of base and exchange of N_2 against triflate, generating the activated acetonitrile−triflate complex **7**. This is the catalytically active species, which is protonated by the parent Mo−NNH_2 acetonitrile complex **3**, generating the alkylimido species **9** and an acetonitrile−N_2 complex **4**, which re-forms the activated complex by exchange of N_2 against triflate. As this complex is constantly regenerated by the educt, the whole reaction can also be described as *autocatalytic*.

An attempt to deprotonate the final product **10** with NEt_3 was unsuccessful, suggesting that the protonation of the coordinated acetonitrile is *irreversible*. This is in sharp contrast to the protonation of coordinated N_2 to NNH_2, which can be reversed by the addition of base (Scheme 2). Importantly, the irreversibility of the nitrile protonation ensures that the overall reaction proceeds quantitatively, although the catalytically active species may be present only in small amounts.

2.4. Reaction of $[Mo(N_2H_2)(dppe)_2(OTf)](OTf)$ (13) with Base. Reaction of the NNH_2 dppe complex $[Mo(N_2H_2)(dppe)_2(OTf)](OTf)$ (**13**) with base (e.g., Et_3N) in acetonitrile leads to formation of the dinitrogen complex $[Mo(N_2)(CH_3CN)(dppe)_2]$ (**14**), in which acetonitrile is coordinated *trans* to the dinitrogen ligand (Scheme 1). This complex was isolated and characterized using various spectroscopic techniques. The infrared spectrum of **14** shows intense bands at 2199 cm^{-1} for the C≡N stretch of coordinated acetonitrile and at 1919

(18) (a) Wagner, G.; Haukka, M.; Fraústo da Silva, J. J. R.; Pombeiro, A. J. L.; Kukushkin, V. Yu. *Inorg. Chem.* **2001**, *40*, 264. (b) Wagner, G.; Pombeiro, A. J. L.; Kukushkin, V. Yu. *J. Am. Chem.* Soc. **2000**, *122*, 3104. (c) Michelin, R. A.; Mozzon, M.; Bertani, R. *Coord. Chem. Rev.* **1996**, *147*, 299. (d) Hegedus, Louis S.; Mulhern, T. A.; Asada, H. *J. Am. Chem. Soc.* **1986**, *108*, 6224.

Scheme 4

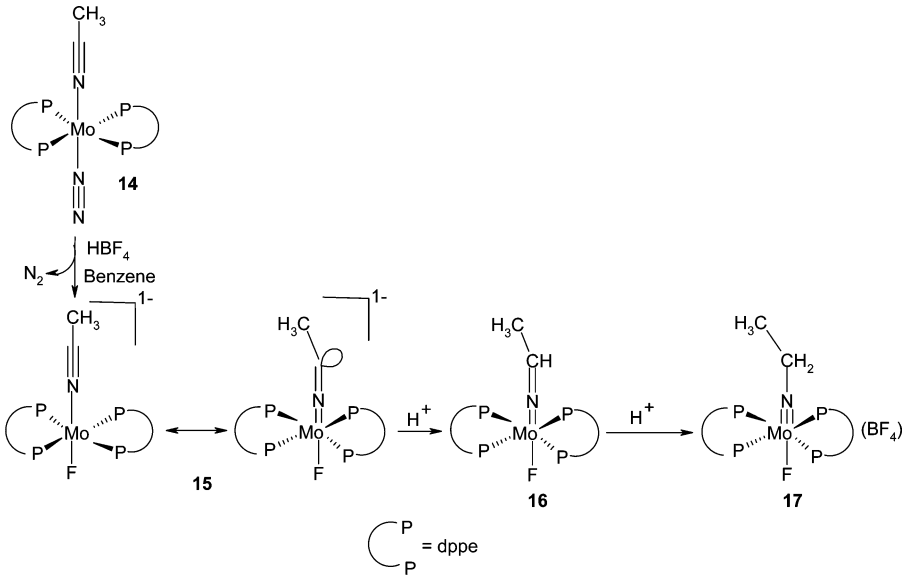

cm^{-1} for the N_2 stretch (Table 2). The simultaneous presence of acetonitrile and dinitrogen in the complex is also evidenced by the Raman spectrum, which shows a strong signal at 2210 cm^{-1} for the C≡N stretch and another broad signal at 1913 cm^{-1} for the N−N stretch (Table 2). Proton NMR of **14** in C_6D_6 shows a single peak at δ 0.98 for the methyl protons of CH_3CN, a peak at 2.35 ppm for the CH_2 protons of dppe, and peaks ranging from 6.89 to 7.67 ppm for the aromatic protons of dppe (Table 1 and Figure S3 (a)). These spectral data are similar to those of $[W(N_2)(CH_3CN)(dppe)_2]$.[12] $^{31}P\{^1H\}$ NMR of **14** in C_6D_6 shows a single peak at δ 59.9 ppm for the four equivalent phosphorus atoms of dppe (Figure S3 (b)), low-field shifted with respect to the corresponding tungsten complex (33.6 ppm).[12]

2.5. Reaction of $[M(N_2)(CH_3CN)(dppe)_2]$ (M = Mo, W) with HBF_4 and CF_3SO_3H. Reaction of $[Mo(N_2)(CH_3CN)(dppe)_2]$ (**14**) with tetrafluoroboric acid in benzene leads to formation of the ethylimido complex $[MoF(NCH_2CH_3)(dppe)_2][BF_4]$ (**17**) (Scheme 1), in analogy with the W system investigated by Field et al.[12] The formation of complex **17** was confirmed by various spectroscopic techniques. Proton NMR in CD_2Cl_2 shows a triplet at −0.19 ppm for CH_3CH_2CN, a quartet at 1.83 ppm for CH_3CH_2CN, and peaks at 2.60 and 2.71 ppm for the CH_2 protons of the dppe ligand. Peaks corresponding to the phenyl protons from the dppe ligands range from 6.86 to 7.43 ppm (Table 1 and Figure S4 (a)). $^{31}P\{^1H\}$ NMR of **17** shows a peak at δ 46.45 ppm for the four phosphorus atoms of the dppe ligand (Table 1 and Figure S4 (b)). ^{19}F NMR indicates a chemical shift of δ −148.31 for the coordinated fluorine atom and a chemical shift of −77.86 ppm for the unbound BF_4^- counterion. The coordinated and noncoordinated fluorine atoms are less shielded than in the $[WF(NCH_2CH_3)(dppe)_2][BF_4]$ complex, where they are observed at −174.8 and −149.9 ppm, respectively.[12]

In analogy with the depe system, formation of the alkylimido complex **17** by protonation of the acetonitrile−N_2 complex **14** with HBF_4 can be explained as follows (Scheme 4): Attack of HBF_4 on complex **14** leads to replacement of N_2 by fluoride, forming the anionic intermediate $[MoF(NCCH_3)(dppe)_2]^-$ (**15**). The binding of fluoride increases the charge donation from the central atom to acetonitrile (vide infra). In analogy with the OTf system the transferred electron density is localized on the β-carbon of the ligand, initiating protonation to form the Mo(IV) ethylimido complex **17**. This reaction proceeds via the Mo(II) azavinylidene complex **16**, in which two-electron transfer from the metal has occurred. In the final, diprotonated complex **17** the metal has transferred four electrons to the acetonitrile ligand. The proposed mechanism is supported by theoretical calculations presented in the following sections.

Reaction of the tungsten analogue of **14**, $[W(N_2)(CH_3CN)(dppe)_2]$ (**14a**), with triflic acid produced the corresponding NNH_2 complex, showing that in this case the dinitrogen ligand of **14a** and not the acetonitrile ligand is protonated. This result indicates that the activation of nitrile in the putative $[W(CH_3CN)(OTf)(dppe)_2]^-$ intermediate (analogous to the depe complex **7**) is not sufficient to ensure its protonation. Thus dinitrogen protonation prevails in this system.

3. Electronic Structure Calculations

3.1. $[Mo(H_2P-CH_2-CH_2-PH_2)_2(CH_3CN)(N_2)]$ (4′) and Derived Complexes. To theoretically study the protonation of acetonitrile on a Mo center, we first consider the starting complex $[Mo(depe)_2(CH_3CN)(NNH_2)]^{2+}$ (**3**), in which acetonitrile is coordinated *trans* to the NNH_2 ligand. DFT calculations carried out for the model system $[Mo(CH_3CN)(NNH_2)(PH_3)_4]^{2+}$ showed that the β-carbon of the acetonitrile in the optimized geometry carries a positive charge (+0.56), and there is no significant change in bond distances (C≡N = 1.175 Å, C_β−C = 1.461 Å) and angles (N−C_β−C = 179.8°) of acetonitrile when compared to the free ligand;[7] hence it is not activated in complex **3** (Tables 3 and 4). Similar results are obtained for model system **4′** of the N_2 complex $[Mo(depe)_2(CH_3CN)(N_2)]$ (**4**), in which acetonitrile is coordinated *trans* to dinitrogen (Figure 4, Table 3). The third possibility is that $[Mo(depe)_2(CH_3CN)(N_2)]$ (**4**) loses dinitrogen to give the square pyramidal intermediate $[Mo(depe)_2(CH_3CN)]$ (**5**). The charge at C_β (+0.28) in the corresponding model system **5′** (Figure

Table 3. Optimized Bond Distances (Å) and Bond Angles (deg) of the Model Systems 4′−7′ and 15′−19′[a]

model system	Mo−N_{an}	C≡N_{an}	C_β−C	Mo−N	Mo−P	N_{an}−C_β−C	Mo−N−C_β	N−Mo−N_{an}
$[Mo(PH_3)_4(NNH_2)(CH_3CN)]^{2+}$ (ref 7)	2.275	1.175	1.461		2.609	179.82	179.73	
CH_3CN		1.160	1.461			180.0		
$[Mo(L)_2(CH_3CN)(N_2)]$ (**4′**)	2.133	1.169	1.459	2.039 1.133 (N≡N)	2.434	179.72	179.48	179.86
$[Mo(L)_2(CH_3CN)]$ (**5′**)	2.044	1.174	1.459		2.422	179.36	179.54	
$[Mo(L)_2(CH_3CN)_2]$ (**6′**)	2.113	1.172	1.458		2.424	179.82	179.82	
$Mo(L)_2(CH_3CN)(OTf)]^-$ (**7′**)	1.990	1.202	2.395 Mo−O		2.443	139.63	176.56	175.94 O−Mo−N
$[Mo(L)_2(CH_3CN)(CH_3{-}CH_2N)]^{2+}$ (**10′**)	2.237 *1.726*	1.160 *1.438*	1.456 *1.535*		2.545	179.87 *112.79*	179.78 *179.47*	
$[Mo(L)_2(F)(CH_3CN)]^-$ (**15′**)	1.99	1.21	1.493	2.228 Mo−F		133.92	176.28	
$[Mo(L)_2(F)(CH_3CHN)]$ (**16′**)	1.890	1.283	1.573	2.078	2.472	123.64	173.22	177.99 F−Mo−N
$[Mo(L)_2(F)(CH_3CH_2N)]^+$ (**17′**)	*1.756*	*1.433*	*1.535*	1.995	2.533	112.61	179.60	179.29
$[Mo(PH_3)_4(CH_3CNH)]^+$ (**18′**)	2.133 2.113 (Mo−C_β)	1.246	1.510		2.463	133.38	72.04	
$[Mo(PH_3)_4(CH_3CHNH)]^{2+}$ (**19′**)	2.109	1.296	1.485		2.553 2.473	125.44	133.30	

[a] L = $H_2P{-}(CH_2)_2{-}PH_2$, an = acetonitrile, numbers in italics are for Mo−NEt.

Table 4. NPA Charge Distribution of Model Systems 4′−7′ and 15′−17′[a]

system	Mo	N	C_β	C	X	ref
$[Mo(PH_3)_4(NCCH_3)(NNH_2)]^{2+}$	−0.02	−0.50	0.56		N_α −0.10 N_β −0.58	7 *
$[Mo(L)_2(NCCH_3)(N_2)]$ (**4′**)	−1.10	−0.33	0.35	−0.78	N_α −0.02 N_β −0.08	
$[Mo(L)_2(NCCH_3)]$ (**5′**)	−0.88	−0.32	0.28	−0.77		*
$[Mo(L)_2(NCCH_3)_2]$ (**6′**)	−1.16	−0.32 −0.32	0.33 0.33	−0.77 −0.77		*
$[Mo(L)_2(NCCH_3)(OTf)]^-$ (**7′**)	−0.93	−0.31	0.11	−0.74	−0.82 (OTf)	*
$[Mo(L)_2(CH_3CN)(CH_3{-}CH_2N)]^{2+}$ (**10′**)	−0.07	−0.21 *−0.47*	−0.31 *+0.52*	−0.68 *−0.81*		*
$[Mo(L)_2(NCCH_3)(F)]^-$ (**15′**)	−0.83	−0.36	0.05	−0.73	−0.63 (F)	*
$[Mo(L)_2(NCHCH_3)(F)]$ (**16′**)	−0.34	−0.41	−0.08	−0.71	−0.58 (F)	*
$[Mo(L)_2(NCH_2CH_3)(F)]^+$ (**17′**)	0.07	−0.35	−0.30	−0.68	−0.56 (F)	*

[a] X = ligand *trans* to the acetonitrile. *This work. Numbers in italics are for acetonitrile. L = $H_2P{-}CH_2{-}CH_2{-}PH_2$.

4) shows that there is a small charge transfer from the metal center to acetonitrile, which is correlated with a reduction of charge density on the Mo center from −1.10 to −0.88 (Table 4). This small reduction of positive charge on the β-carbon is certainly not sufficient for protonation of this atom. In a fourth possibility the acetonitrile from the reaction medium can occupy the vacant site in the five-coordinate intermediate **5** to give the six-coordinated complex $[Mo(depe)_2(CH_3CN)_2]$ (**6**). NPA charge analysis of the corresponding model system **6′** (Figure 4) shows that there is again a positive charge (+0.33) on the β-carbon of acetonitrile (Table 4); therefore this ligand is not activated. *Thus the β-carbon of actonitrile is not activated in all of the above four possible intermediates.* This is supported by the structural parameters collected in Table 3.

The final possibility is that OTf replaces the dinitrogen ligand of **4** to give $[Mo(depe)_2(CH_3CN)(OTf)]^-$ (**7**), in which acetonitrile is coordinated *trans* to the OTf ligand (Scheme 2). This intermediate is examined in the next section.

3.2. $Mo(H_2P{-}CH_2{-}CH_2{-}PH_2)_2(CH_3CN)(OTf)]^-$ (7′) and $[Mo(H_2P{-}CH_2{-}CH_2{-}PH_2)_2(F)(CH_3CN)]^-$ (15′). Geometry optimization of model system $[Mo(H_2P{-}CH_2{-}CH_2{-}PH_2)_2(CH_3CN)(OTf)]^-$ (**7′**) shows that the Mo−N_{an} (an = acetonitrile) bond distance (1.990 Å) gets shorter than a Mo−N_{an} single bond (compare the other model systems in Table 3), whereas the C−N triple bond is elongated to 1.202 Å. More importantly, the acetonitrile ligand bends at C_β (N−C_β−C angle 139.63°), which has not been observed for any other model system (Table 3). The geometry change of acetonitrile from linear to bent reflects a charge transfer from the central ion to the ligand, changing the hybridization of the β-carbon of acetonitrile from sp to sp^2.

As shown in Section 2.5, the reaction of HBF_4 with $[Mo(dppe)_2(CH_3CN)(N_2)]$ (**14**) in benzene generates the acetonitrile-protonated and not the dinitrogen-protonated product. In analogy with the OTf system, anion binding should be the reason for this finding. To check this assumption, the OTf ligand in model system **7′** was replaced by fluoride, leading to structure $[Mo(H_2P{-}CH_2{-}CH_2{-}PH_2)_2(CH_3CN)(F)]^-$ (**15′**). Initially the bond angle at C_β was set to 180° and bond distances and angles for rest of the atoms were set to the values of the parent dinitrogen complex (**14**). In the course of optimization the Mo−N bond distance of acetonitrile was found to shorten from 2.379 Å to 1.99 Å and the N≡C bond distance to elongate from 1.161 Å to 1.21 Å. Most importantly, the bond angle of $CH_3{-}C{\equiv}N$ was reduced from 180.0° to 133.0° (Table 3, Figure 4), similar to what is observed for the OTf complex **7′**.

Natural population analysis (NPA, Table 4) shows that the positive charge on the β-carbon of nitrile decreases from +0.35 in the dinitrogen complex to +0.11 (OTf complex **7′**) and +0.05 (F complex **15′**), whereas

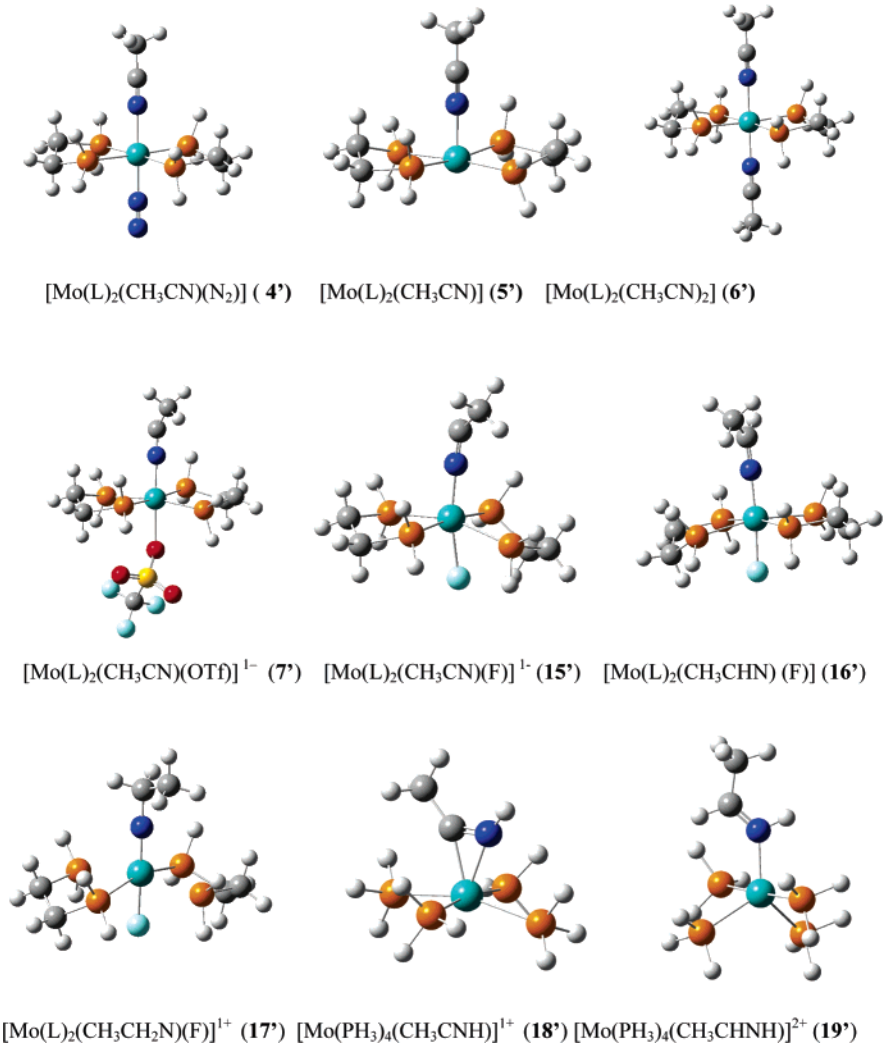

Figure 4. Optimized structures of the model systems (L = $H_2P-CH_2-CH_2-PH_2$).

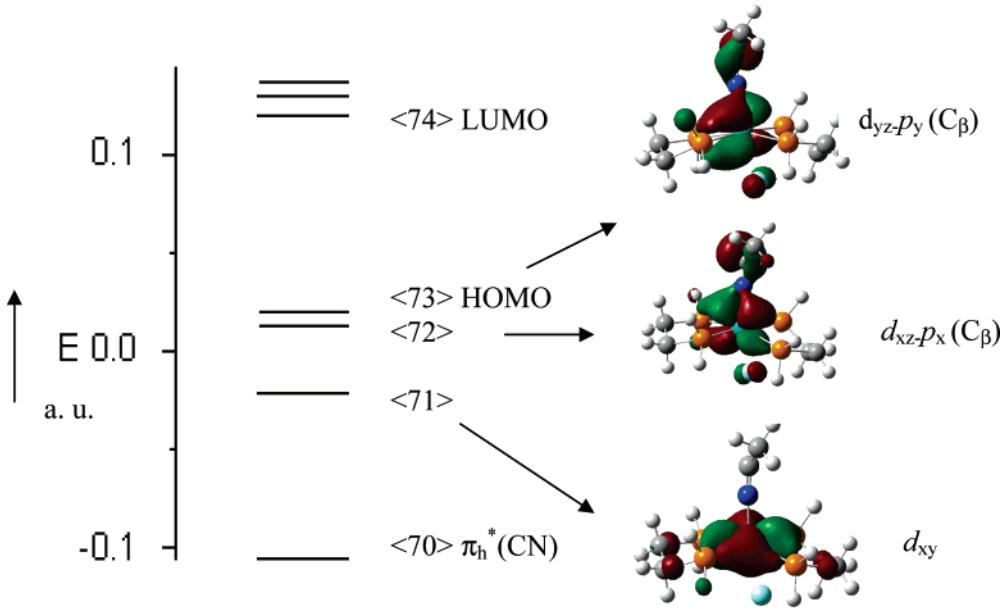

Figure 5. MO scheme of $[Mo(H_2P-CH_2-CH_2-PH_2)_2(CH_3CN)(F)]^-$ (**15′**).

the nitrogen atom of nitrile carries a charge of −0.31 (OTf complex) and −0.35 (F complex). The molecular orbital calculation of model system **15′** reveals that the HOMO has metal−fluoride and β-carbon lone-pair character (13%; Table 5 and Figure 5). In contrast, the contribution of N_α in the highest occupied orbitals of **15′** is small; the same applies to the OTf complex **7′**. In the following, the fluoro complex [Mo($H_2P-CH_2-CH_2-$

Table 5. Charge Decomposition and Energies for Important Molecular Orbitals of the Model Systems 15′−17′

				orbital decompositions					
system	orbital no.	orbital description	energ (a u)	%Mo	%N	%C_β	%C_γ	%F	%P
15′ Mo(0) d^6	⟨68⟩		−0.134	11.56	5.85	0.59	0.31	58.77	15.64
	⟨69⟩		−0.120	10.97	1.82	1.35	0.07	31.97	45.04
	⟨70⟩		−0.105	5.75	1.34	0.91	0.13	35.46	45.60
	⟨71⟩	d_{xy}	−0.021	59.39	0.42	1.01	0.01	0.31	9.69
	⟨72⟩	$d_{xz}-p_x(C_\beta)$	0.013	48.81	1.67	12.89	4.08	4.09	10.00
	⟨73⟩	HOMO,$d_{yz}-p_y(C_\beta)$	0.019	55.01	1.37	8.44	2.16	5.33	8.72
	⟨74⟩		0.119	56.70	0.27	0.50	0.21	0.20	23.48
	⟨75⟩		0.130	50.79	3.05	2.14	12.94	0.67	21.62
	⟨76⟩		0.136	64.40	2.80	1.60	4.77	0.08	19.32
	⟨77⟩		0.149	14.92	1.72	0.63	1.27	1.98	36.98
	⟨78⟩		0.165	47.12	2.75	4.46	1.23	0.82	18.01
16′ Mo(II) d^4	⟨68⟩		−0.292	12.23	9.84	0.50	0.33	66.26	5.98
	⟨69⟩		−0.256	8.16	5.91	0.62	2.40	12.04	58.41
	⟨70⟩		−0.253	5.34	4.26	3.31	0.26	25.72	51.72
	⟨71⟩		−0.209	17.21	34.15	0.34	7.74	12.26	17.40
	⟨72⟩	d_{xy}	−0.172	70.72	0.35	0.97	0.02	0.07	5.64
	⟨73⟩	HOMO,$d_{xz}-p_x(C_\beta)$	−0.130	57.34	0.26	18.40	0.24	8.52	4.56
	⟨74⟩	LUMO,$d_{yz}-p_y(C_\beta)$	−0.020	43.94	15.78	2.37	9.94	3.82	10.26
	⟨75⟩		0.002	43.83	0.20	0.52	0.14	0.28	28.58
	⟨76⟩		0.015	8.84	1.59	0.18	0.18	2.23	33.56
	⟨77⟩		0.016	53.99	0.25	0.75	0.43	0.18	30.83
	⟨78⟩		0.027	24.43	0.02	0.04	0.01	0.00	68.12
17′ Mo(IV) d^2	⟨68⟩		−0.436	23.94	0.01	2.98	0.01	0.01	49.40
	⟨69⟩		−0.412	15.62	15.32	4.94	2.18	1.44	43.47
	⟨70⟩		−0.404	17.09	23.04	0.94	4.30	0.16	38.72
	⟨71⟩	$p_x(N)-d_{xz}$	−0.385	15.37	21.39	2.60	0.60	21.53	28.60
	⟨72⟩	$p_y(N)-d_{yz}$	−0.380	12.23	16.93	0.79	2.24	18.46	40.06
	⟨73⟩	HOMO, d_{xy}	−0.330	80.64	0.32	0.66	0.02	0.01	3.38
	⟨74⟩	LUMO, $d_{xz}-p_x(N)$	−0.167	41.43	21.02	0.66	2.03	3.75	18.42
	⟨75⟩	$d_{yz}-p_y(N)$	−0.159	46.26	21.15	1.00	5.35	3.61	13.93
	⟨76⟩		−0.134	31.35	0.11	0.14	0.01	0.24	61.43
	⟨77⟩		−0.125	25.79	0.16	2.02	0.37	3.29	36.76
	⟨78⟩		−0.120	32.90	0.78	0.40	0.41	0.11	31.36

$PH_2)_2(F)(CH_3CN)]^-$ (**15′**) is treated as a generic model system to study the stepwise protonation of organonitriles.

3.3. Monoprotonated Intermediate [$Mo^{II}(H_2P-CH_2-CH_2-PH_2)_2(F)(CH_3CHN)$] (16′). Structure [$Mo(H_2P-CH_2-CH_2-PH_2)_2(F)(CH_3CHN)$] (**16′**) of the monoprotonated intermediate (methyl−azavinylidene complex) was optimized at the same level of theory as employed in the previous calculations. The optimized structural parameters are given in Table 3. In **16′** the Mo−F and Mo−N interactions become stronger than in **15′**, as evident from the shortening of these two bonds in comparison to the parent structure. The N−C bond distance, in contrast, is elongated and is now comparable to a double bond (Table 3). The N−C−C bond angle is slightly reduced to 123.64° and the F−Mo−N bond angle stays close to linear (Table 3).

Natural population analysis (NPA) of **16′** (Table 4) shows that the β-carbon now carries a charge of −0.08. Addition of one proton on the β-carbon of acetonitrile thus has increased the negative charge on this center, concomitant with a reduction of electron density on the metal from −0.83 to −0.34. Selected orbitals of **16′** are shown in Figure 6. The HOMO (⟨73⟩) is a Mo d_{xz} orbital (57.34% Mo, 8.52% F) with a contribution of an out-of-plane p orbital (18.40%) at the β-carbon. The LUMO corresponds to the HOMO (d_{yz}) of the acetonitrile complex **15′**, reflecting a two-electron oxidation of the molybdenum center to Mo(II) (d^4) (Table 5). The electron density transferred from the metal center is localized on the C_β atom of the ligand. The lone pair at C_β thus can interact with another proton to give the doubly protonated product **17′**.

3.4. Fluoro Ethylimido Complex [$Mo^{IV}(H_2P-CH_2-CH_2-PH_2)_2(F)(CH_3CH_2N)]^+$ (17′) and Acetonitrile Ethylimido Complex [$Mo(H_2P-CH_2-CH_2-PH_2)_2(NCH_2CH_3)(CH_3CN)]^{2+}$ (10′). The geometry of the (doubly protonated) ethylimido model system **17′** was optimized at the same level as the other structures; important bond distances and angles are given in Table 3. The Mo−N (acetonitrile) bond distance now is close to a Mo≡N distance, and the N−C_β distance is elongated to a value close to a N−C single bond. There is a slight change in the Mo−F bond distance as compared to model system **16′** (Table 3). Selected molecular orbitals are shown in Figure 7. The HOMO is the nonbonding orbital d_{xy}. The LUMO corresponds to the HOMO of the monoprotonated complex **16′**, reflecting another two-electron oxidation of the molybdenum center to Mo(IV) (d^2). LUMO and LUMO+1 are metal-centered orbitals (d_{xz} and d_{yz}) that have an antibonding interaction with the p_x and p_y orbitals of the β-carbon of acetonitrile, respectively (Figure 7 and Table 5). Similar results are obtained for the complex [$Mo(depe)_2(NCH_2CH_3)(CH_3CN)](OTf)_2$ (**10**), which is generated from **17′** through replacement of OTf by acetonitrile (Schemes 1 and 2). Selected bond distances and angles of 10′ are listed in Table 3; contours are shown in Figure 8. As observed for model system **17′**, the HOMO is the nonbonding d_{xy} orbital. LUMO and LUMO+1 are d_{xz} and d_{yz} orbitals

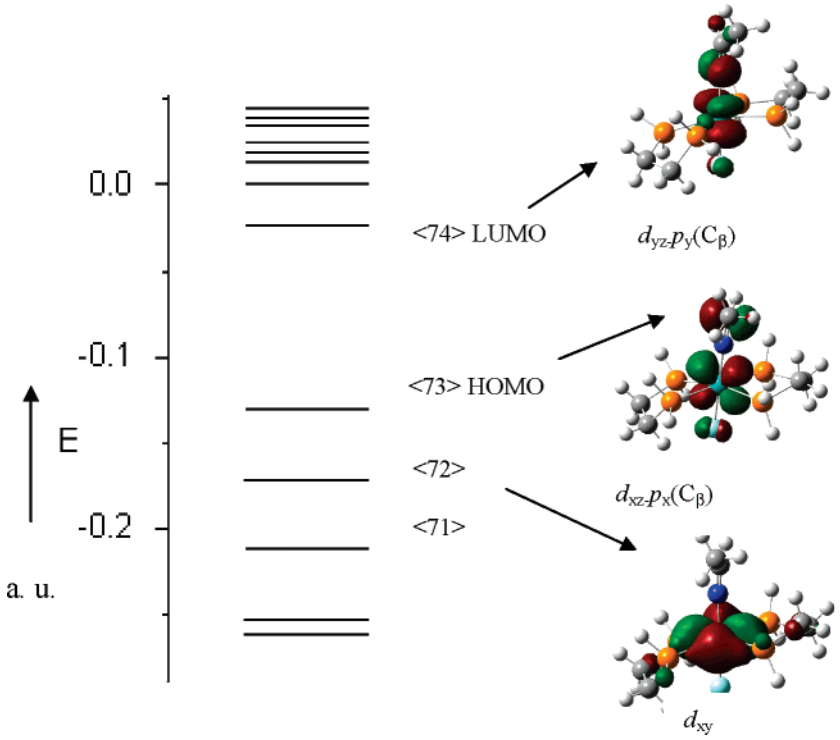

Figure 6. MO scheme of [Mo($H_2P-CH_2-CH_2-PH_2)_2$(NCHCH$_3$)(F)] (**16′**). A Mo(II) d^4 configuration applies.

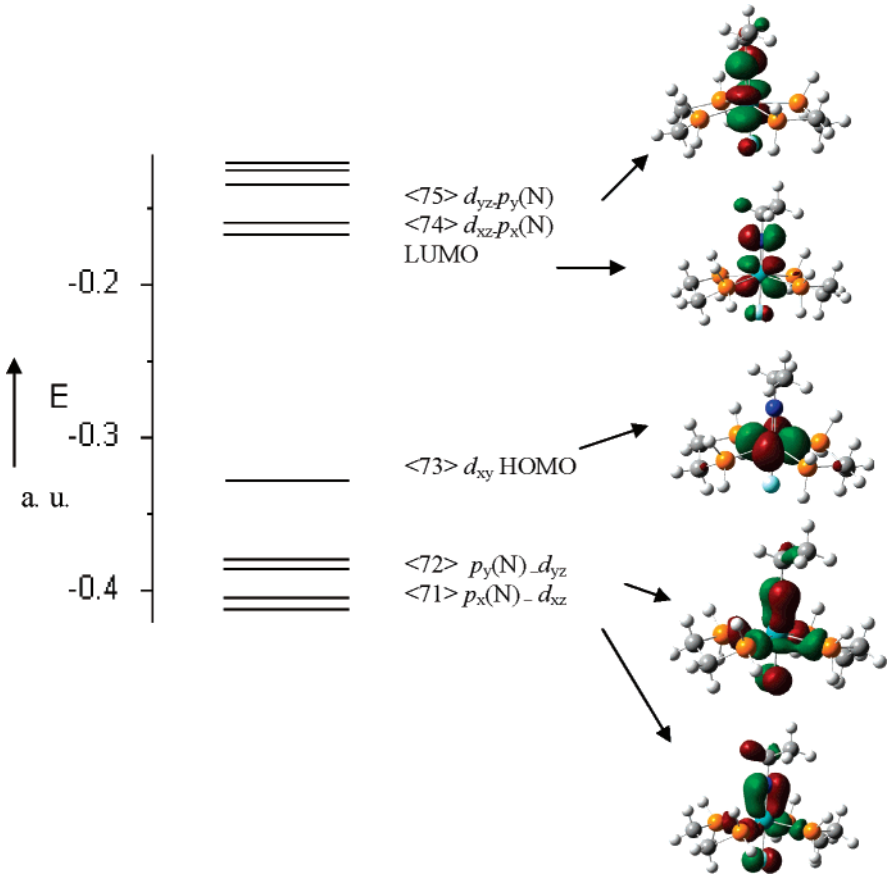

Figure 7. MO scheme of the [Mo($H_2P-CH_2-CH_2-PH_2)_2$(NCH$_2$CH$_3$)(F)]$^+$ (**17′**). A Mo(IV) d^2 configuration applies.

that have an antibonding interaction with NEt and a bonding interaction with the acetonitrile ligand, again reflecting a Mo(IV) oxidation state of the central atom.

3.5. Energetics of the Proposed Reaction Path. To check the feasibility of the proposed reaction mechanism, an energy profile was determined (Figure 9 and Table 6). Loss of N_2 from the acetonitrile−dinitrogen complex **4′** is associated with a standard free enthalpy change of +18.7 kcal/mol (Figure 9, left). The subsequent bonding of triflate to the five-coordinate intermediate **5′** leading to **7′** is also endergonic (+16.9 kcal/

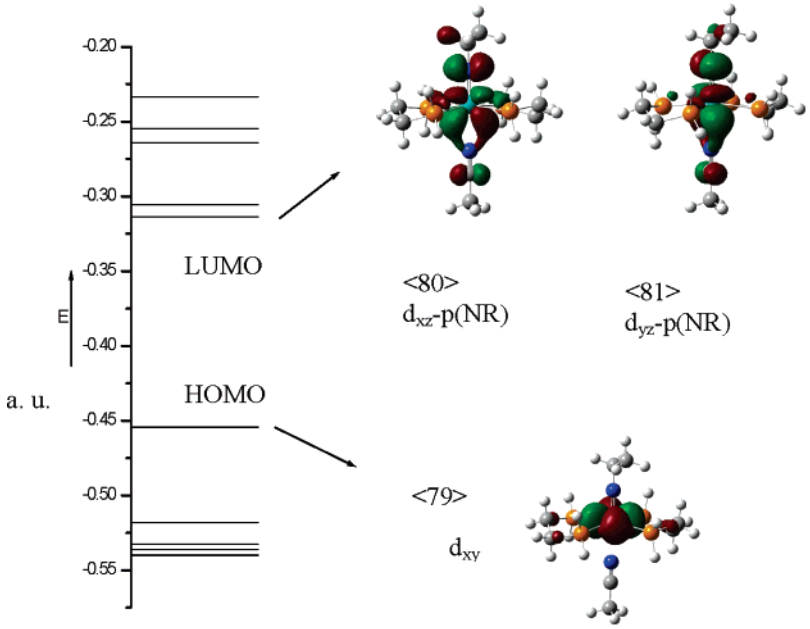

Figure 8. Molecular orbital scheme of the model system $[Mo(H_2P-CH_2-CH_2-PH_2)_2(CH_3CN)(CH_3CH_2N)]^+$ (**10′**).

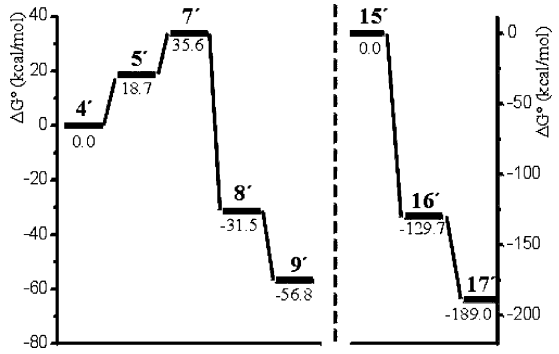

Figure 9. Protonation of triflate (left) and fluoro (right) acetonitrile complexes. All energies correspond to standard free enthalpies and are in kcal/mol.

mol), but the subsequent protonation of C_β is strongly exergonic (−67.1 kcal/mol). For the corresponding fluoro complex **15′**, the first protonation is exergonic by −129.7 kcal/mol (Figure 9, right). The apparent barrier for this process (+35.6 kcal/mol for the triflate system, cf. Figure 9, left) is effectively lowered by the fact that **4′** loses dinitrogen to the atmosphere, generating (under argon) a sufficient concentration of the five-coordinate intermediate **5′**.[28] This will bind triflate in a moderately endergonic reaction, leading to the monoprotonated intermediate **8′**. The strongly exergonic character of the latter step ensures the irreversibility of the entire reaction course.

3.6. Examination of Primary Protonation at N_α. As an alternative to the proposed scenarios, initial protonation of the coordinated nitrile could in principle also occur at N_α (Scheme 5). We theoretically examined this pathway based on the five-coordinate complex **5**. Protonation of the nitrile nitrogen atom first leads to the side-on-coordinated intermediate **18** (cf. Supporting Information). Further protonation of **18** at C_β then forms the coordinatively unsaturated ketimine complex **19**, which adds another ligand X (OTf or fluoride), leading to **20**. To generate the observed alkylimido products **9** and **17**, respectively, this complex has to rearrange, either by a direct proton shift from the imine N to C_β or (more probably) by a deprotonation/reprotonation process via the azavinylidene intermediates **8** and **16**, respectively. Although this scenario is in principle possible, it does not explain the differences observed between the depe system **3** and the dppe system **13** upon reaction with base (nitrile protonation vs lack of nitrile activation; cf. Scheme 1). Furthermore, the different protonation pathways observed for the acetonitrile−dinitrogen complexes $[M(dppe)_2(N_2)(CH_3CN)]$ (M = Mo,

(19) Horn, K. H.; Lehnert, N.; Tuczek, F. *Inorg. Chem.* **2003**, *42*, 1076.
(20) Becke, A. D. *J. Chem. Phys*. **1993**, *98*, 5648.
(21) Dunning, T. H., Hay, P. J., Schaefer, H. F, Eds. *Modern Theoretical Chemistry*; Plenum: New York, 1976.
(22) Petersson, G. A.; Al-Laham. A. *J. Chem. Phys*. **1991**, *94*, 6081.
(23) (a) Schaefer, A.; Horn, H.; Ahlrichs, R. *J. Chem. Phys.* **1992**, *97*, 2571. (b) Schaefer, A.; Hubner, C.; Ahlrichs, R. *J. Chem. Phys.* **1994**, *100*, 5829.
(24) (a) Cancès, M. T.; Mennucci, B.; Tomasi, J. *J. Chem. Phys.* **1997**, *107*, 3032. (b) Cossi, M.; Barone, V.; Mennucci, B.; Tomasi, J. *Chem. Phys. Lett.* **1998**, *286*, 253. (c) Mennucci, B.; Tomasi, J. *J. Chem. Phys.* **1997**, *106*, 5151.
(25) Reed, A. E.; Curtis, L. A.; Weinhold, F. *Chem. Rev.* **1988**, *88*, 899. (b) Reed, A. E.; Weinhold, F. *J. Am. Chem. Soc.* **1986**, *108*, 3586. (c) Reed, A. E.; Weinstock, R. B.; Weinhold. F. *J. Chem. Phys.* **1985**, *83*, 735. (d) Reed, A. E.; Winhold, F. *J. Chem. Phys*. **1983**, *83*, 1736.
(26) Frisch, M. J.; Trucks, G. W.; Schlegel, H. B.; Scuseria, G. E.; Robb, M. A.; Cheeseman, J. R.; Montgomery, J. A., Jr.; Vreven, T.; Kudin, K. N.; Burant, J. C.; Millam, J. M.; Iyengar, S. S.; Tomasi, J.; Barone, V.; Mennucci, B.; Cossi, M.; Scalmani, G.; Rega, N.; Petersson, G. A.; Nakatsuji, H.; Hada, M.; Ehara, M.; Toyota, K.; Fukuda, R.; Hasegawa, J.; Ishida, M.; Nakajima, T.; Honda, Y.; Kitao, O.; Nakai, H.; Klene, M.; Li, X.; Knox, J. E.; Hratchian, H. P.; Cross, J. B.; Adamo, C.; Jaramillo, J.; Gomperts, R.; Stratmann, R. E.; Yazyev, O.; Austin, A. J.; Cammi, R.; Pomelli, C.; Ochterski, J. W.; Ayala, P. Y.; Morokuma, K.; Voth, G. A.; Salvador, P.; Dannenberg, J. J.; Zakrzewski, V. G.; Dapprich, S.; Daniels, A. D.; Strain, M. C.; Farkas, O.; Malick, D. K.; Rabuck, A. D.; Raghavachari, K.; Foresman, J. B.; Ortiz, J. V.; Cui, Q.; Baboul, A. G.; Clifford, S.; Cioslowski, J.; Stefanov, B. B.; Liu, G.; Liashenko, A.; Piskorz, P.; Komaromi, I.; Martin, R. L.; Fox, D. J.; Keith, T.; Al-Laham, M. A.; Peng, C. Y.; Nanayakkara, A.; Challacombe, M.; Gill, P. M. W.; Johnson, B.; Chen, W.; Wong, M. W.; Gonzalez, C.; Pople, J. A. *Gaussian 03*, Revision B.04; Gaussian, Inc.: Pittsburgh, PA, 2003.
(27) Neese, F. *ORCA*, version 2.2; Max-Planck Institut für Bioanorganische Chemie: Mühlheim/Ruhr, Germany, 2004.
(28) This hypothesis is supported by the fact that the reaction proceeds slower under dinitrogen than under argon.

Table 6. Energies and Thermochemical Data of the Model Systems

system	energy [hartree]	ZPE + thermal correction [hartree]	entropy [cal/mol K]	ΔG_{solv}[c] [kcal/mol]	$G°$ [kcal/mol]	$\Delta G°$ [kcal/mol]
$[Mo(CH_3CN)(N_2)]$ (**4′**)	−5747.66857494	0.267178	148.706	+6.60	−3606586.99	0[a]
$[Mo(CH_3CN)]$ (**5′**)	−5638.05229405	0.256376	145.504	+6.83	−3537807.32	+18.67[a]
$[Mo(CH_3CN)(OTf)]^-$ (**7′**)	−6599.84194930	0.293095	190.040	−21.37	−4141357.98	+35.59[a]
$[Mo(CH_3CHN)(OTf)]^-$ (**8′**)	−6600.41808753	0.307779	185.630	+7.98	−4141679.63	−31.46[a]
$[Mo(CH_3CH_2N)(OTf)]^+$ (**9′**)	−6600.83158869	0.321379	180.697	−22.50	−4141959.57	−56.80[a]
N_2	−109.56669572	0.008472	45.885	+1.59	−68761.00	
OTf^-	−961.767733	0.035384	85.515	−45.74	−603567.58	HOTf → OTf^- $\Delta G = 254.60$
HOTf	−962.253602	0.045640	86.893	−1.47	−603822.18	
$[Mo(CH_3CN)(F)]^-$ (**15′**)	−5738.01181798	0.257620	149.889	−18.64	−3600558.87	0[b]
$[Mo(CH_3CHN)(F)]$ (**16′**)	−5738.61965457	0.272423	151.433	+0.72	−3600912.11	−129.66[b]
$[Mo(CH_3CH_2N)(F)]^+$ (**17′**)	−5739.05892992	0.287569	151.220	−16.09	−3601195.00	−188.97[b]
ether	−233.749360	0.143810	79.769	−0.87	−146614.50	$etherH^+$ → ether $\Delta G = 223.58$
$etherH^+$	−234.076363	0.157085	82.408	−26.79	−146838.08	

[a] Relative to **4′** + free OTf^-. [b] Relative to **15′** taking consumed $etherH^+$ molecules into account. When employing a solution of HBF_4 in ether, the protonating agent is a protonated ether. [c] In all calculations involving triflic acid solv = acetonitrile; in all calculations involving HBF_4, solv = benzene.

Scheme 5

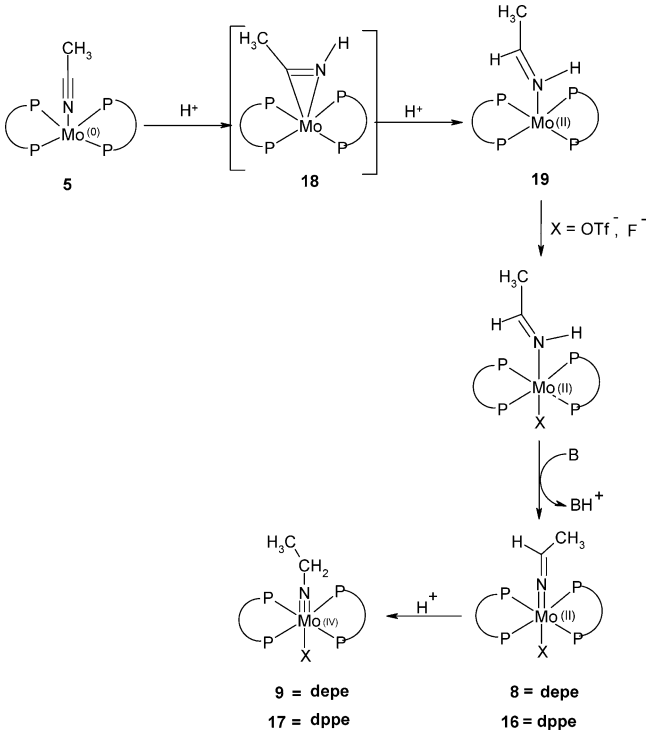

W; HBF_4: nitrile protonation; CF_3SO_3H: dinitrogen protonation) would not be understandable. These experimental observations rather suggest a *synergistic activation* of nitrile by the anionic Lewis base (triflate, fluoride) and the phosphine ligation (dppe, depe), which is not needed in Scheme 5, but is necessary in the β-protonations described Schemes 2−4. We thus conclude that initial protonation at N_α is not important in the conversion of nitriles to alkylimides.

4. Discussion

In the preceding sections the conversion of a Mo(IV) acetonitrile−NNH_2 complex with depe coligands (**3**) to a Mo(IV) ethylimido complex (**10**) + N_2 has been described. The reaction was discovered when we tried to adapt the method of Field et al.[12] for the preparation of *trans* W dppe dinitrogen−acetonitrile complexes to the corresponding depe systems. Upon addition of base to the NNH_2−acetonitrile complex **3**, however, the expected dinitrogen complex **4** was not formed, but instead the ethylimido complex **10** was obtained. By reduction of the amount of base it was then established that only catalytic amounts of base are necessary to start the reaction. Upon treatment with base, the $[Mo(NNH_2)(CH_3CN)(dppe)_2]$ complex **13**, in contrast, was found to give the corresponding dinitrogen complex **14**, which could not be isolated in the depe system. Subsequent addition of HBF_4 to complex **14** then generates the ethylimido complex **17**, in agreement with the literature.[12,15]

The observed protonation of coordinated acetonitrile at a Mo(0)−N_2 fragment with diphos coligands is remarkable, as DFT predicts a fairly large positive charge at the β-carbon of acetonitrile (+0.35), which should render protonation of this atom rather unfavorable. This even more applies to the NNH_2 complex $[Mo(NNH_2)(CH_3CN)(dppe)_2]^{2+}$ (+0.56; Table 4). In this respect, it is noteworthy that the NNH_2 depe complexes **2** ($[Mo(NNH_2)(OTf)(depe)_2](OTf)$) and **3** ($[Mo(NNH_2)(CH_3CN)(depe)_2](OTf)_2$) also spontaneously convert to the ethylimido complex **10** + N_2 in acetonitrile. These autocatalytic conversions, however, take more time for completion than the base-catalyzed reaction, indicating that deprotonation of the NNH_2 complexes to give the dinitrogen intermediate **4** is essential for the reaction (Schemes 2 and 4). However, acetonitrile does not appear to be activated in this complex either (vide supra). N_2 therefore has to displaced or exchanged against a stronger activating ligand. By exclusion of all other possibilities, this can only be triflate, leading to the six-coordinate, anionic Mo(0) complex **7**. On the basis of the significantly lowered positive charge on C_β (+0.11) and the bending at C_β, acetonitrile in fact appears to be activated toward protonation in **7**. The feasibility of the proposed reaction pathway was demonstrated by an energy profile that shows that the involved intermediates are thermally accessible. In a strongly exergonic reaction, the activated complex **7** abstracts a proton from the parent NNH_2 complex **3** to give a monoprotonated Mo(II) azavinylidene complex **8**,

which, however, cannot be isolated.[29] Further protonation of **8** leads to the Mo(IV) alkylimido complex **9**. Deprotonation of the NNH_2 complex by these reactions leads to the dinitrogen complex **4**. The dinitrogen ligand in **4** can again be replaced by OTf, re-forming complex **7**; in this way a cyclic reaction course ensues (Scheme 4). The OTf ligand in complex **9** readily undergoes replacement with acetonitrile to give complex **10**, which is isolated as the final product.

Whereas the depe dinitrogen−acetonitrile complex **4** is unstable toward protonation of coordinated acetonitrile, it is possible to isolate the dinitrogen−acetonitrile dppe complex $[Mo(dppe)_2(N_2)(CH_3CN)]$ (**14**) by deprotonation of its NNH_2 analogue **13** (vide supra). It can be anticipated that the $[Mo(dppe)_2(N_2)(CH_3CN)]$ (**14**) complex undergoes the same ligand displacement reactions as its depe counterpart. In particular, an activated acetonitrile−triflate complex like **7** may form if OTf^- is present in solution, *but for dppe this species does not appear to mediate protonation of the bound acetonitrile to generate the corresponding alkylimido complex*. This finding would once more reflect the differences in the electronic donor/acceptor properties of depe and dppe; that is, depe is a stronger σ-donor than dppe, whereas the latter is a stronger π-acceptor. As a consequence, the triflate depe complex **7** mediates protonation of the bound acetonitrile, whereas the activation of nitrile provided by the analogous triflate dppe complex is not sufficient. Nevertheless, the actonitrile−N_2 dppe complex **14** allows protonation of the coordinated acetonitrile using HBF_4 as acid (Scheme 4). In the framework of the proposed reaction scheme, this suggests that binding of a *stronger Lewis base than triflate* (such as fluoride) is required to activate acetonitrile on a Mo(0) *dppe* complex. This is supported by DFT calculations, which indicate a stronger charge transfer to acetonitrile and a stronger exergonicity of the protonation reactions by $[MoF(diphos)_2]^-$ than by $[Mo(OTf)(diphos)_2]^-$. On the other hand, if triflic acid is used to protonate the tungsten dppe complex $[W(dppe)_2(N_2)(CH_3CN)]$, then not acetonitrile but dinitrogen is protonated. These findings demonstrate that the activation of nitrile is a combined effect of the phosphine ligation and the Lewis-basic coligand.

5. Experimental Section

General Procedures. All syntheses were carried out in an atmosphere of dinitrogen or argon using standard Schlenk techniques. All solvents were dried over appropriate drying agents under an inert atmosphere. $MoCl_5$, dppe, and depe were purchased from Aldrich. $[Mo(N_2H_2)(depe)_2(OTf)](OTf)$ (**2**) and $[Mo(N_2H_2)(dppe)_2(OTf)](OTf)$ (**12**) were synthesized using literature procedures.[16] MIR spectra were recorded from KBr pellets using a Mattson Genesis Type I spectrometer. Raman spectra were recorded on a Bruker IFS 66/CS NIR spectrometer. NMR spectra were recorded on a Bruker Avance 400 pulse Fourier transform spectrometer operating at a ^1H frequency of 400.13 MHz, ^{31}P 161.98 MHz, and ^{19}F 376.50 MHz using a 5 mm inverse triple-resonance probe head. References as substitutive standards: H_3PO_4 85% pure, δ (^{31}P) = 0 ppm, and $CFCl_3/CDCl_3$, δ (^{19}F) = 0 ppm, were used.

Synthesis of $[Mo(N_2H_2)(depe)_2(CH_3CN)](OTf)_2$ (3). A 0.300 g sample of complex **2** was transferred into a 250 mL three-necked round-bottomed flask; 100 mL of acetonitrile was added and the mixture stirred for 6 h. The solution was concentrated to 10 mL, and diethyl ether was added. Complex **3** was precipitated out in a quantitative yield. IR (KBr): 1326 ((s), N=NH_2), 2278 (s, C≡N), 3095, 3253 (w(br), NH_2) cm^{-1}. ^1H NMR (C_6D_6): δ 2.13 (m, PCH_2CH_2P), 2.18 (s, CH_3CN), 7.52 (s, 2H, NH_2) ppm. $^{31}P\{^1H\}$ NMR (C_6D_6): δ 44.5. Anal. Found: C, 32.52; H, 5.86; N, 4.49. Calcd for $C_{24}H_{53}N_3P_4S_2O_3F_6Mo$: C, 32.84; H, 6.08; N, 4.78.

Synthesis of $[Mo(depe)_2(NCH_2CH_3)(CH_3CN)](OTf)_2$ (10). A catalytic amount of NEt_3 was added to 0.300 g of $[Mo(N_2H_2)(depe)_2(CH_3CN)](OTf)_2$ (**3**) complex in 100 mL of acetonitrile solution. This solution was stirred for 1 h and concentrated to 10 mL under vacuum. Diethyl ether was added to this solution, and complex **10** was precipitated out. Yield: 94%. IR (KBr): 2280 (w(br), C≡N). Raman: 2272 (w(br), C≡N). ^1H NMR (C_6D_6): δ 1.20 (t, 3H, CH_3CH$_2$N), 1.81 (m, 4H, PCH_2CH_2P), 2.1 (s, CH_3CN), 1.94 (q, 2H, CH$_3$CH_2N) ppm. $^{31}P\{^1H\}$ NMR (C_6D_6): δ 59.9. Anal. Found: C, 34.82; H, 6.08; N, 3.08. Calcd for $C_{26}H_{56}N_2P_4S_2O_3F_6Mo$: C, 35.06; H, 6.29; N, 3.14.

Reaction of $[Mo(N_2H_2)(dppe)_2(OTf)](OTf)$ (12) with Base. Et_3N (0.23 mmol) was added to a solution of $[Mo(N_2H_2)(dppe)_2(OTf)](OTf)$ (**12**) (0.2 mmol) complex in acetonitrile (20 mL), and the reaction mixture was stirred at room temperature for 30 min. The resulting dark red precipitate was separated by filtration, washed with acetonitrile, and dried in vacuo to give $[Mo(N_2)(CH_3CN)(dppe)_2]$ (**14**) as a red solid (73%). IR (KBr): 2199 (w(br), C≡N), 1919 (w(br), N_2) cm^{-1}. Raman: 2201 (w(br), C≡N), 1913 (w(br), N_2) cm^{-1}. ^1H NMR (C_6D_6): δ 0.98 (s, 3H, CH_3CN), 2.35 (m, 8H, PCH_2CH_2P), 6.89−7.67 (m, 40H, P(C_6H_5)$_2$) ppm. $^{31}P\{^1H\}$ NMR (C_6D_6): δ 59.9. Anal. Found: C, 67.13; H, 5.13; N, 4.21. Calcd for $C_{54}H_{51}N_3P_4Mo$: C, 67.43; H, 5.34; N, 4.36.

Reaction of $[Mo(N_2)(CH_3CN)(dppe)_2]$ (14) with HBF_4. Tetrafluoroboric acid (0.28 mmol) was added to a solution of $[Mo(N_2)(CH_3CN)(dppe)_2]$ (**14**) (0.24 mmol) in benzene (20 mL), and the reaction mixture was stirred at room temperature for 2 h and filtered through a sintered-glass frit. The filtrate was concentrated, and the addition of ether precipitated a yellow solid, which was separated by filtaration and washed with diethyl ether (2 × 10 mL) to give a yellow solid of $[MoF(NCH_2CH_3)(dppe)_2][BF_4]$ (**17**) (62%). ^1H NMR ($CDCl_3$): δ −0.19 (t, 3H, CH_3CH$_2$N), 1.83 (dq, 2H, CH$_3$CH_2N), 2.60 (m, 4H, PCH_2CH_2P), 2.71 (m, 4H, PCH_2CH_2P), 6.86−7.43 (m, 40H, P(C_6H_6)$_2$) ppm. $^{31}P\{^1H\}$ NMR ($CDCl_3$): δ 46.45. ^{19}F NMR ($CDCl_3$): δ −148.31 (1F, MoF), −77.86 (4F, BF_4^-) ppm. Anal. Found: C, 62.04; H, 5.03; N, 1.13. Calcd for $C_{54}H_{53}BF_5NP_4Mo$: C, 62.26; H, 5.12; N, 1.34.

Reaction of $[W(N_2)(CH_3CN)(dppe)_2]$ (14a) with CF_3SO_3H. Triflic acid (0.37 g, 0.27 mmol) was added to a solution of $[W(N_2)(CH_3CN)(dppe)_2]$ (0.12 g, 0.11 mmol) in benzene (25 mL), and the reaction mixture was stirred at room temperature for 3 h and filtered through a sintered-glass frit. The filtrate was concentrated, and upon addition of ether an orange-yellow solid precipitated. The solid was separated by filtration (G4) and washed with diethyl ether (3 × 10 mL) to give an orange-yellow mixture of $[W(NNH_2)(OTf)(dppe)_2][OTf]$ (**20**) and $[W(NNH_2)(CH_3CN)(dppe)_2][OTf]_2$ (**21**) (57%, 3:1, respectively). The ratio of the complexes is identified on the basis of NMR peak integrations. Complex **20**: ^1H NMR ($CDCl_3$): δ 2.59 (m, 4H, PCH_2CH_2P), 3.18 ((m, 4H, PCH_2CH_2P)), 6.18 (b, NH_2), 7.10−7.39 (m, 40H, P(C_6H_6)$_2$) ppm. $^{31}P\{^1H\}$ NMR ($CDCl_3$): δ 42.21. ^{19}F NMR ($CDCl_3$): δ −78.75 (3F, OTf), −76.67 (3F, Mo−OTf). Complex **21**: IR (KBr): 2269 (w(br), C≡N), 3235, 3344 (w(br), NH_2) cm^{-1}. ^1H NMR ($CDCl_3$): δ 2.15 (s, CH_3CN), 2.59 (m, 4H, PCH_2CH_2P), 2.81 ((m, 4H, PCH_2CH_2P)), 6.18 (b, NH_2), 7.10−7.39 (m, 40H, P(C_6H_6)$_2$) ppm. $^{31}P\{^1H\}$ NMR ($CDCl_3$): δ 38.95. ^{19}F NMR ($CDCl_3$): δ −78.75 (6F, OTf).

DFT Calculations. The structures of model systems **4′**−**10′** and **15′**−**19′** have been fully optimized using Becke's three-

(29) The azavinylidene product could be isolated and characterized in a $[Re(I)Cl(dppe)_2]$ complex; see ref 14b.

parameter hybrid functional with the LYP correlation functional of Lee, Yang, and Parr.[20] The LANL2DZ basis set was used for the metal center, and 6-31G* was used for the nonmetal centers.[21,22] N_2, HOTf, OTf^-, Et−O−Et, and Et−OH−Et^+ were optimized using the B3LYP functional together with the TZVP[23] basis set. Vibrational frequency calculations have been performed on these optimized structures to obtain the corresponding entropy, ZPE, and thermal correction data. A solvent correction calculation (acetonitrile and benzene,respectively) was also performed using the polarized continuum model (PCM).[24] Charges were calculated using the natural bond orbital (NBO) formalism.[25] All these computational procedures were used as they are implemented in the Gaussian-03 package.[26] Wave functions were plotted using Gaussview 03. To obtain reliable single-point energies for **4′**−**5′**, **7′**−**9′**, and **15′**−**17′**, single-point calculations have been performed on the optimized structures using the B3LYP functional together with the larger TZVP basis set as implemented in ORCA.[27]

Acknowledgment. F.T. and C.S. thank DFG Tu58/12 and FCI for funding of this research.

Supporting Information Available: ^{1}H NMR and ^{31}P NMR spectra of complexes **3**, **10**, **14**, and **17** as well as optimized Cartesian coordinates of the model systems. This material is available free of charge via the Internet at http://pubs.acs.org.

OM050220R